Anomalous scaling of low-order structure functions of turbulent velocity

By S. Y. CHEN[1], B. DHRUVA[2], S. KURIEN[3], K. R. SREENIVASAN[4], and M. A. TAYLOR[5]

[1]Department of Mechanical Engineering, Johns Hopkins University, Baltimore, MD 21218, USA

[2]Schlumberger-Doll, Ridgefield, CT, USA

[3]Center for Nonlinear Studies (CNLS) and Mathematical Modeling & Analysis Group (T7), Los Alamos National Laboratory, Los Alamos, NM 87505, USA

[4]International Center for Theoretical Physics, Strada Costiera 11, 34014 Trieste, Italy

[5]Computer and Computational Sciences (CCS-3), Los Alamos National Laboratory, Los Alamos, NM 87505, USA

(Received 27 May 2004and in revised form ??)

It is now believed that the scaling exponents of moments of velocity increments are anomalous, or that departures from Kolmogorov's (1941) self-similar scaling increase nonlinearly with the increasing order of the moment. This appears to be true whether one considers velocity increments themselves or their absolute values. However, moments of order lower than 2 of the absolute values of velocity increments have not been investigated thoroughly for anomaly. Here, we discuss the importance of the scaling of non-integer moments of order between +2 and -1, and obtain them from direct numerical simulations at moderate Reynolds numbers and experimental data at high Reynolds numbers. The relative difference between the measured exponents and Kolmogorov's prediction increases as the moment order decreases towards -1, thus showing that anomaly, which is manifest in high-order moments, is evidently present in low-order moments as well. This result provides a motivation for seeking a theory of anomalous scaling as the order of the moment vanishes. Such a theory does not have to consider rare events—which may be affected by non-universal features such as shear—and so may be regarded as advantageous to consider and develop.

1. Introduction

The moments of velocity differences over spatial scales of size r, the so-called structure functions, provide useful measures of the statistical description of fluid turbulence (Kolmogorov (1941a), Kolmogorov (1941b)). In particular, the longitudinal structure functions, defined as

$$S_n(\mathbf{r}) = \left\langle [(\mathbf{u}(\mathbf{x}+\mathbf{r}) - \mathbf{u}(\mathbf{x})) \cdot \hat{\mathbf{r}}]^n \right\rangle, \tag{1.1}$$

have been studied extensively. Here, $\mathbf{u}(\mathbf{x})$ is the velocity vector at position $\mathbf{x}$, and $\hat{\mathbf{r}}$ is the unit vector along the separation vector $\mathbf{r}$. The special interest in structure functions comes in part from an exact result, known as the 4/5-ths law,

$$S_3(\mathbf{r}) = -\frac{4}{5}\epsilon r, \tag{1.2}$$

valid in the inertial range of scales ($\eta \ll r \ll L$ where η is the Kolmogorov scale characterizing the dissipative scale of motion and L is a suitable large scale of turbulence). In part, the interest is spurred by the operational ease with which longitudinal structure functions can be obtained from experimental data if one makes the so-called Taylor's hypothesis (Taylor (1935)). The major impetus for measurements, however, is the scaling result of Kolmogorov—K41 for brevity—that, for Reynolds numbers, the structure functions follow the relation $S_n(\mathbf{r}) \sim r^{\zeta_n}$ where the scaling exponent $\zeta_n = n/3$. As a result of considerable work (see, for example, Anselmet et al. (1984), Maurer et al. (1994), Arneodo et al. (1996), Sreenivasan & Antonia (1997), it now appears nearly certain that the scaling exponents deviate from $n/3$ increasingly and nonlinearly as n increases. This is the anomalous scaling. While some issues remain to be explained satisfactorily (see, for example, Sreenivasan & Dhruva (1998)), it appears that anomalous scaling is a genuine result worthy of a serious theoretical effort. Consequently, sizeable thrusts of research have occurred in this direction (e.g., L'vov & Procaccia (1996)).

One obvious concern about high-order moments is that, since they sample the tails of the probability distribution function (PDF) of velocity increments—and since some of the associated rare events may be tied to well-defined flow structures in real space—it is not clear that the results for high-order moments are unambiguously universal: this is so because the mean shear and other non-universal features driving the flow could influence flow structures that are rare. In contrast, low-order moments are less susceptible to such non-universal properties, because they are determined nearly entirely by the core of the PDF and hence sampled frequently. Thus, it is reasonable to regard anomalous scaling—and its universality—as more conclusively established if low-order moments also display anomaly. This is the main concern of this paper.

The lowest non-trivial moment that has been studied extensively is the second-order structure function, whose scaling exponent has been shown to be ≈ 0.7. Though this is different from the predicted value of $2/3$, the difference is too small to be conclusive on its own. It would thus be useful to examine scaling exponents for moments of still lower orders. Since moments of order -1 and below do not exist for velocity increments (Castaing et al. 1990), our range of interest is limited to $-1 < n \leqslant 2$, where n is necessarily fractional. With decreasing n in this range, if the deviation from $n/3$ decreases, we shall at least know that K41 will be exact in the limit of low-order moments, and regard it as a possible reference point for a theory. If, on the other hand, these deviations remain to be non-trivial as n vanishes, it may well be that the understanding of the anomaly can be sought more fruitfully in terms of low-order moments, for the simple reason that such a theory can justifiably ignore structures in real space and other rare events. Some preliminary measurements were published in Sreenivasan et al. (1996) and Cao et al. (1996) but the present paper is a more complete examination of the data. Perhaps more importantly, the preliminary numbers did not take account of the possible effects of residual anisotropy in both experiments and simulations. We do so here using a recently developed angle-averaging technique (Taylor et al. (2003)).

The rest of the paper is organized as follows. In section 2, we describe the experimental and numerical data used for the present analysis. This is followed in section 3 by the calculation of the fractional structure functions and their scaling exponents from the datasets described in section 2. For the 1024^3 simulations, we eliminate possible effects of residual anisotropy by angle-averaging. The exponents from the various sources of data are in good agreement with each other and deviate measurably from the K41 prediction even as $n \to 0$. Section 4 contains a brief discussion of the significance of the results.

U	u′	ϵ	η	λ	R_λ
7.6 ms^{-1}	1.36 ms^{-1}	0.032 $\mathrm{m}^2\mathrm{s}^{-3}$	0.57 mm	11.4 mm	10,340

TABLE 1. Some relevant parameters for the atmospheric data. Here, U is the mean speed, u′ is the root-mean-square velocity, ϵ is the mean rate of energy dissipation, η and λ are the Kolmogorov and Taylor microscales, respectively, and $R_\lambda \equiv u'\lambda/\nu$, ν being the kinematic viscosity of air at the temperature of the measurement.

2. Experimental and numerical data

2.1. *High-Reynolds number atmospheric boundary layer measurements*

Hotwire measurements were made in the atmospheric surface layer at a height of 35 m above the ground using the meteorological tower at Brookhaven National Laboratory. The tower itself presented very little obstacle to the wind because of its low solidity. The dataset analyzed here is part of a more comprehensive batch of data obtained at the tower. The hotwire, 0.7 mm in length and 0.5 μm in diameter, was placed facing the wind, about two meters away from the tower. (For monitoring the wind direction, the tower was equipped with a vane anemometer placed two meters away from the measurement station.) The calibration was performed in situ using a TSI calibrator and checked later in a windtunnel. The signals were low-pass filtered at 5 kHz and sampled at 10 kHz. The anemometer and signal conditioners were placed nearby at the height of measurement, and the conditioned signal was transmitted to the ground and digitized using a 12-bit A/D converter. Typical data records contained between 10 and 40 million samples, during which time the wind direction and its mean speed were deemed acceptably constant. More details are given in Dhruva (2000), but the essential features for this particular set of data are listed in table 1. The wind conditions were somewhat unstable.

2.2. *Two direct numerical simulations of Navier-Stokes equations with forcing*

The Navier-Stokes equations were solved numerically for periodic boundary conditions. A pseudospectral code was used using a second-order time-integration scheme Cao et al. (1996). Simulations were carried out with a resolution of 512^3 grid points on the CM-5 at Los Alamos national Laboratory and SP machines at IBM Watson Research Center. To obtain a statistically steady state, a forcing is applied to the first wave-number shells $0.5 < k < 1.5$ so that at each time step the total energy of that shell is constant. Time integration up to 60 large-eddy turn-over times was performed to collect data for statistical analysis.

Even though the numerical data show well-developed scaling range in an ESS plot, the Reynolds number is not large enough to produce unambiguous scaling in direct log-log plots of moments versus the scale r. The computational grid was 512^3 in size and, as already remarked, the maximum microscale Reynolds number was about 250. It was also found that, even though the turbulence is nominally isotropic, there are some measurable (though small) differences between the scaling of longitudinal and transverse structure functions, suggesting a possible presence of residual anisotropy in the inertial range, arising from forcing anisotropy. For these two reasons, it seemed worthwhile to consider data from a higher Reynolds number simulations and ensure that anisotropy effects, if they are present at all, could be accounted for in a rational manner. We therefore used the velocity data from a simulation of the Navier-Stokes equation in a periodic domain of size 1024^3. The forcing scheme is similar to that described above for the 512^3 simulation and is explained in detail in Taylor et al. (2003). In this case the steady state was achieved

N	ν	ϵ	$\frac{\delta x}{\eta}$	R_λ
1024	3.5×10^{-5}	1.75	0.75	450

TABLE 2. Some relevant parameters for the 1024^3 DNS.

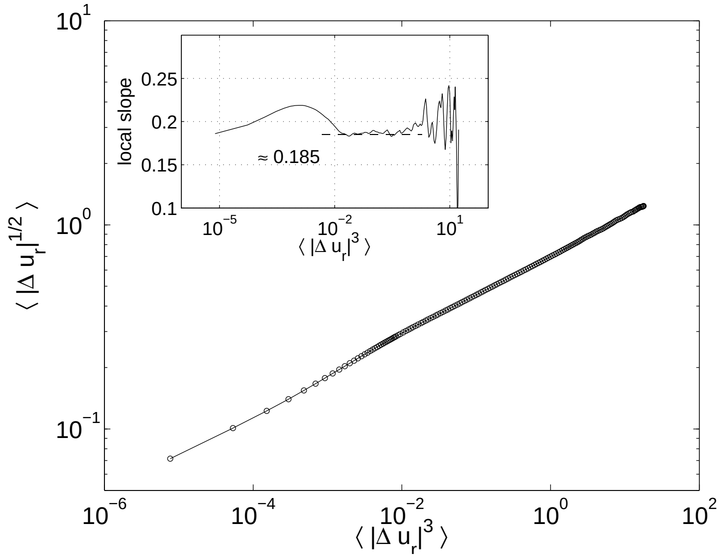

FIGURE 1. ESS calculation of scaling exponent of order 0.5 from experimental data.

in about 1.5 large-eddy turnover times and the simulation ran for a total of 2.5 large-eddy turnover times. The statistical analysis was performed over 10 frames in the final eddy turnover time. The steady state Taylor-microscale Reynolds number was $R_\lambda \sim 450$. Other parameters of this simulation are given in Table 2.

3. Results

Since we are interested in real-valued structure functions, we can consider, when the moment order is either fractional or negative, only the moments of absolute values of velocity differences defined as

$$S_{|n|}(\mathbf{r}) = \left\langle \left| (\mathbf{u}(\mathbf{x}+\mathbf{r}) - \mathbf{u}(\mathbf{x})) \cdot \hat{\mathbf{r}} \right|^n \right\rangle. \tag{3.1}$$

where n may be a fraction or a negative integer. In experimental measurements, because the Reynolds number is quite high (see table 1), and hence the scaling ranges reasonably clear, we have the luxury of estimating the scaling exponent directly from log-log plots of $S_{|n|}(\mathbf{r})$ versus r (see Dhruva (2000)).

We also performed the calculation using extended self-similarity or ESS (Benzi et al. (1993)). In ESS, the structure function $S_n(\mathbf{r})$ of interest is plotted against another structure function $S_m(\mathbf{r})$ and the relative scaling exponent ζ_n/ζ_m is obtained. In particular, if the exponent of $S_m(\mathbf{r})$ is known *a priori*, as from the theoretical estimate for the third-order structure function (Eq. 1.2), then the exponent of $S_n(\mathbf{r})$ may be inferred. It is known that ESS improves the scaling range significantly. In the present case we use $S_m(\mathbf{r}) = S_{f3}(\mathbf{r})$, the absolute third-order structure function and assume its scaling expo-

order of moments	measured exponents	relative difference	DNS exponents (512^3)	relative difference	DNS exponents (1024^3)	relative difference
-0.80	-0.317	0.189	-0.313	0.174	-	-
-0.60	-	-	-	-	-0.238±0.002	0.188
-0.40	-	-	-	-	-0.158±0.001	0.181
-0.20	-0.078	0.170	-0.077	0.155	-0.078±0.001	0.171
0.10	0.039	0.170	0.036	0.080	0.039±0.001	0.155
0.20	0.076	0.140	0.073	0.095	0.077±0.001	0.152
0.30	0.113	0.130	0.112	0.120	0.115±0.001	0.147
0.40	0.150	0.125	0.150	0.125	0.152±0.001	0.143
0.50	0.187±0.003	0.140	0.187	0.122	0.190±0.001	0.138
0.60	0.221	0.105	0.223	0.115	0.226±0.001	0.133
0.70	0.265	0.136	0.260	0.114	0.263±0.001	0.128
0.80	0.292	0.095	0.296	0.110	0.300±0.001	0.123
0.90	0.333	0.110	0.332	0.107	0.340±0.001	0.119
1	0.372	0.116	0.366	0.098	0.370±0.006	0.111
1.25	0.458	0.099	0.452	0.085	0.459±0.006	0.101
1.50	0.542	0.084	0.536	0.072	0.545±0.006	0.091
1.75	0.628	0.077	0.619	0.061	0.630±0.006	0.079
2.00	0.704±0.003	0.061	0.699	0.049	0.712±0.006	0.064

TABLE 3. Scaling exponents from ESS compared with those from for isotropic turbulence from two sets DNS data. Error bars are given for the experimental data for two exponents. Those for the 512^3 data are given in Cao et al. (1996).

nent is 1. There is some current discussion as to whether this assumption is valid since the K41 theory does not make any mention of the moments of absolute differences, and indeed it appears that the scaling exponents of S_3 and $S_{|n|}$ are in fact slightly different (Sreenivasan et al. (1996)). However, we found that the exponents obtained from ESS were within uncertainty of those obtained directly by Dhruva (2000). An example of ESS plot for moment-order of 0.5 is shown in figure 1, along with the local slope (see inset).

For the numerical simulation data with resolution of 512^3, the exponents were obtained by ESS because the scaling region was small in direct log-log plots against the scale r. Both sets of exponents are listed in table 3.

3.1. *Effects of finite Reynolds number and anisotropy*

The finite Reynolds number of turbulence in numerical work shortens the inertial range over which clear scaling exponents may be observed. This remains a constraint because the applicable theory concerns the limit of Re $\rightarrow \infty$. A constraint in experimental data is that some large-scale anisotropy might be present in the range that appears to be scaling. This effect could be present even in high-Reynolds-number flows because the effects of anisotropic forcing penetrate the scaling range in a subtle but systematic way Arad, L'vov & Procaccia (1999), Kurien & Sreenivasan (2001). In numerical simulations, the statistics are usually calculated in the coordinate directions of the flow (that is, for $\hat{\mathbf{r}}$ oriented parallel to a box-side). If there is persistent anisotropy (angular-dependence) of the statistics in the small-scales, then looking in only a few directions might bias the results. Since we are concerned here with delicate results, this source of uncertainty due to anisotropy has to be addressed satisfactorily.

3.1.1. *Recovering isotropic statistics by angle-averaging*

We make use of two recent developments to properly eliminate the effect of anisotropy in the inertial range in our final data set, the 1024^3 numerical simulation. First, we now know that isotropic and anisotropic contributions can be isolated systematically by projecting structure function of a given order over a particular basis function in its SO(3) group decomposition (Arad et al. (1998), Kurien et al. (2000), Kurien & Sreenivasan (2000), Arad et al. (1999), Warhaft & Chen (2001)). This is a useful step to perform even in nominally isotropic turbulence because the effect of forcing might persist in the nominal scaling range. Second, the recent work by Taylor et al. (2003) developed a method by which the third-order longitudinal structure function was computed in *many* directions of the flow; the results were then averaged over all angles for a given r. The angle-averaged value of the structure function achieved the Kolmogorov 4/5 prediction to a remarkable degree, thus providing a convincing method for extracting the isotropic component of an arbitrary anisotropic flow. This angle-averaging procedure is in effect a projection onto the isotropic component of the SO(3) rotation group decomposition. The method is independent of the order of the structure function and we use it as described below for the fractional statistics.

The angle-averaged isotropic structure function in the flow domain D is given by

$$S_{|n|}(r) = \frac{1}{\Delta t}\int_{t_0}^{t_0+\Delta t} dt \int \frac{d\Omega_r}{4\pi}\int_D \frac{d\mathbf{x}}{L^3}\left|(\mathbf{u}(\mathbf{x}+\mathbf{r}) - \mathbf{u}(\mathbf{x}))\cdot\hat{\mathbf{r}}\right|^n, \tag{3.2}$$

where the usual average over the domain for a particular direction of the unit separation vector $\hat{\mathbf{r}}$ is followed by a spherical average of all possible orientations of $\hat{\mathbf{r}}$ over the solid angle Ω_r. The long-time average is over times where the flow has reached steady state. In our case t_0 is 1.5 large-eddy turnover times into the simulation, and Δt is 1 large-eddy turnover time.

In numerical simulations, since we have the full three-dimensional velocity field, we can in principle perform the integration over the sphere and so project out the isotropic part of the function. The work of Taylor et al. (2003) showed that the full spherical average may be approximated to arbitrary precision by first computing the structure function over sufficiently many different directions in the flow, interpolating each of these functions by a simple single-variable cubic spline, and then averaging the interpolated values over the all the directions. This angle-averaging of the structure functions is much cheaper to implement than, say, first interpolating the three-dimensional, three-component velocity data over spherical shells in order to perform the integration. It is also more accurate in the small scales than other spherical averaging schemes.

At the very low-order moments $|n| < 1$ we observed that the anisotropy in the inertial range was marginal in the sense that the statistics computed in the different directions nearly coincided with each other with differences observed only at large scales $r/\eta > 300$. Nevertheless, the angle-averaging procedure was performed for all orders and the angle-averaged functions were used to deduce the scaling exponents. In figure 2 we show the logarithmic derivative (the local slope) of the structure functions for various fractional orders, This is just the local scaling exponent $\zeta_{|n|}$ as a function of r. The inertial range scaling is the (mean) value of the local slope function over the range in which it is nearly horizontal. A rough estimate of the inertial range from figure 2 is $50 < r/\eta < 140$ and the error estimate on the value scaling exponent is calculated as the variance over this range. As expected, the smaller the absolute order $|n|$, the flatter is the local-slope function over this range indicating the that our confidence level improves as the order decreases. The scaling exponents and their uncertainty over the inertial range are given for a range of fractional orders in table 3, column 6. The exponents calculated in the three different ways from the three different datasets available display a good degree of agreement.

The scaling exponents computed in this way from the 1024^3 simulation are plotted as a function of order n in figure 3. For comparison, the K41 exponents are also shown.

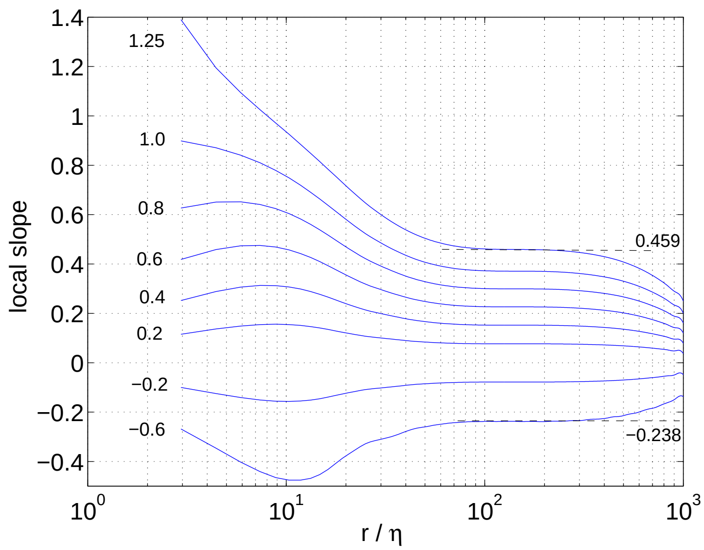

FIGURE 2. The scaling exponents equal to the local slopes $\zeta_{|n|} = d\log(S_{|n|}(r))/d\log(r)$ as a function of r, for various values of $-1 < n < 2$ computed from the 1024^3 DNS. Each curve is labeled on the left by the order of the structure function. The values of the scaling exponents which can be deduced in this way are given on the right for two representative orders, $n = 1.25$ and $n = -0.6$.

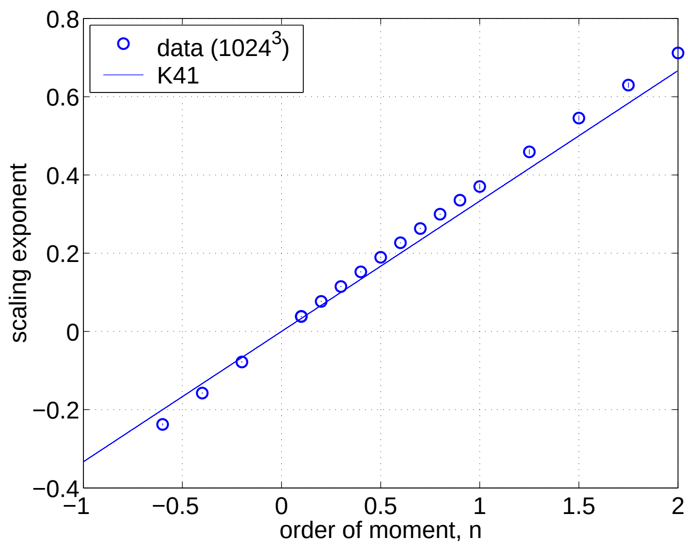

FIGURE 3. The value of scaling exponents calculated from the 1024^3 DNS ($\circ$); standard deviations ($\approx \pm 0.001$) are smaller than the size of the circles. Full line: K41 exponents, extrapolated via self-similarity arguments to the low-order statistics. Anomalous scaling is evident.

The measured exponents deviate from the corresponding K41 exponents at each order. This shows that the intermittency, until now thought to be characteristic of only the high-order moments which sample the 'fat' tails of the PDF of velocity increments, in fact measurably persists into the low-order moments, which sample the core of the PDF. Figure 4 shows the relative departure of the measured scaling exponents from the self-

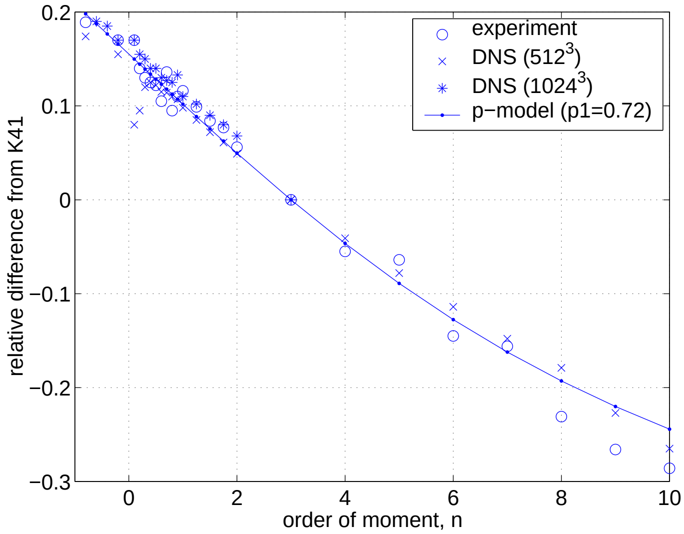

FIGURE 4. The relative difference $(\zeta_{|n|} - n/3)/(n/3)$ for the various $-1 < n \leqslant 10$ as calculated from the experiments ($\circ$), DNS (512^3) ($\times$) and DNS (1024^3) ($\star$). This difference smoothly goes through $n = 0$ without any special feature, suggesting that anomaly is present even in the limit of the zero-th order moment. There is also no special behavior as $n \to -1$ at which point the mathematically defined scaling exponent and hence the relative difference, diverges. The exponents for $n > 3$ for the experiments and the 512^3 simulation are taken from the values tabulated in Dhruva (2000).

similarity prediction of K41, $(\zeta_{|n|} - n/3)/(n/3)$, is a smooth function of n in the range $-1 < n \leqslant 10$ (figure. 4). We have also presented the anomalous exponents calculated from the multifractal p-model for comparison. *More here on the p-model.* The dependence on n in the range $-1 < n \leqslant 3$ is more or less linear and becomes weakly quadratic for $n > 3$. The exact 4/5−law result of K41 with scaling exponent 1, takes the relative difference to zero at $n = 3$. A noteworthy point in this curve is at $n = 0$. The relative difference from K41 is not defined for $n = 0$, nevertheless, the experimental and model values go smoothly through zero. We interpret this to mean that anomalous scaling exists in the limit $n \to 0$ with relative departure from K41 of about 16% (see the y-intercept at $n = 0$ in figure 4). As the negative powers are approached the relative anomaly increases smoothly as $n \to -1$. The negative order moments have negative scaling exponents and hence greater contribution from the small scales than from the large scales when compared to the positive order statistics. *Does that and the following sentence make sense?* This suggests that they are sampling the extremely non-gaussian PDFs of the velocity difference across the very small scales; as one gets closer to $n = -1$ the moments remain formally well-defined, but the finite resolution makes measured moments of order $n < -0.8$ or so increasingly noisy in the small scales.

4. Discussion and conclusions

The principal result of this work is that fractional low-order moments have scaling exponents that are different from $n/3$. In this sense, it is reasonable to consider that anomaly exists in both negative and very low-order moments. Thus, instead of focusing entirely on high-order moments in search of an explanation for intermittency, it may also be reasonable to attempt to understand this feature for low-order moments. This has the advantage that one is focusing not on rare events whose universality may be in some question, unless some additional care is taken.

We should remark on a lingering uncertainty. To keep structure functions real-valued, we can only consider, in the range $-1 < n \leqslant 2$, fractional moments of absolute valued velocity increments defined through (3.1). The difference between the structure functions defined in 1.1 and the corresponding ones defined for absolute-valued velocity increments is by no means clear for large n. An ongoing investigation () appears to indicate that the absolute-valued structure functions have a larger scaling exponent than the classical ones when n is large and odd. It cannot therefore be dismissed entirely that the departures from $n/3$ that one may observe for small and fractional n may merely suggest the possibility that K41 does not somehow apply to absolute moments. Even if this is our only conclusion, it is still new and thus of some interest.

REFERENCES

Anselmet, F., Gagne, F., Hopfinger, E.J. & Antonia, R.A. 1984 High-order velocity structure functions in turbulent shear flow. *J. Fluid Mech.* **140**, 63-89.

Arad, I., Dhruva, B., Kurien, S., L'vov, V.S., Procaccia, I. & Sreenivasan, K.R. 1998 Extraction of anisotropic contributions in turbulent flows. *Phys. Rev. Lett.* **81**, 5330-5333.

Arad, I., L'vov, V.S. & Procaccia, I. 1999 Correlation functions in isotropic and anisotropic turbulence: The role of the symmetry group. *Phys. Rev. E* **59**, 6753-6765.

Arad, I., Biferale, L., Mazitelli, I. and Procaccia, I. 1999 Disentangling scaling properties in anisotropic and inhomogeneous turbulence. *Phys. Rev. Lett.* **82**, 5040-5043.

Arneodo,A.,Baudet, C., Belin, F., Benzi, R., Castaing, B.,Chabaud, B.,Chavarria, R., Ciliberto, S., Camussi, R., Chilla, F., Dubrulle, B., Gagne, Y., Hebral, B., Herweijer, J., Marchand, M., Maurer, J., Muzy, J.F., Naert, A., Noullez, A., Peinke, J., Roux, F., Tabeling, P., van de Water, W. & Willaime, H. 1996 Structure functions in turbulence, in various flow configurations, at Reynolds number between 30 and 5000, using extended self-similarity. *Europhys. Lett.* **34**, 411-416.

Benzi, R., Ciliberto, S., Tripiccione, R., Baudet, C., Massaioli, F. & Succi, S. 1993 Extended self-similarity in turbulent flows. *Phys. Rev. E* **49**, R29-R32.

Cao, N., Chen, S. & Sreenivasan, K.R. 1996 Scaling of low-order structure functions in homogeneous turbulence. *Phys. Rev. Lett.* **77**, 3799-3802.

Castaing, B., Gagne, Y. & Hopfinger, E.J. 1990 Velocity probability density-functions of high Reynolds-number turbulence. Physica D **46**, 177-200.

Dhruva, B. 2000 An experimental study of high-Reynolds-number turbulence in the atmosphere. *Ph.D. thesis, Yale University.*

Kolmogorov, A.N. 1941a The local structure of turbulence in incompressible viscous fluid for very large Reynolds numbers. *Doklad. Akad. Nauk. SSR* **30**. Reproduced in *Proc. Roy. Soc. Lond. A.* **434** 9-13.

Kolmogorov, A.N. 1941b Dissipation of energy in the locally isotropic turbulence. *Doklad. Akad. Nauk. SSR* **32** 16-18. Reproduced in *Proc. Roy. Soc. Lond. A.* 1991 **434** 15-17.

Kurien, S., L'vov, V.S., Procaccia, I. & Sreenivasan, K.R. 2000 Scaling structure of the velocity statistics in atmospheric boundary layers. *Phys. Rev. E* **61**, pp. 407-421.

Kurien, S. & Sreenivasan, K.R. 2000 Anisotropic scaling contributions to high-order structure functions in high-Reynolds-number turbulence. *Phys. Rev. E* **62**, 2206-2212.

Kurien, S. & Sreenivasan, K.R. 2001 Measures of Anisotropy and the universal properties of turbulence *New Trends in Turbulence* Les Houches Summer School 2000 Proceedings, Eds: Lesieur,M., Yaglom, A. & David, F., 55-111.

L'vov, V. & Procaccia, I. 1996 Turbulence: a universal problem. *Phys. World* **9**, 35-40.

Maurer, J., Tabeling, P. & Zocchi, G. 1994 Statistics of turbulence between two counter-rotating disks in low-temperature helium gas. *Europhysics Letters* **26**, 31-36.

Sreenivasan, K.R. & Antonia, R.A. 1997 The phenomenology of small-scale turbulence. *Annu. Rev. Fluid Mech.* **29**, 435-472.

Sreenivasan, K.R. & Dhruva, B. 1998 Is there scaling in high-Reynolds-number turbulence? *Progress of Theoretical Physics Supplement*, **130**, 103-120.

Sreenivasan, K.R., Vainshtein, S.I., Bhiladvala, R., San Gil, I., Chen, S. & Cao, N. 1996 Asymmetry of velocity increments in fully developed turbulence and the scaling of low-order moments. *Phys. Rev. Lett.* **77**, 8-11.

Warhaft, Z. & Shen 2001 Some comments on the small scale structure of turbulence at high Reynolds number. *Physics of Fluids* **13**, 1532-1533.

Taylor, G.I. 1935 Statistical theory of turbulence. I-IV *Proc. Roy. Soc. Lond. A* **151**, 421-478.

Taylor, M.A., Kurien, S. & Eyink, G.L. 2003 Recovering isotropic statistics in turbulence simulations: The Kolmogorov 4/5-th law *Phys. Rev. E* **68**, 26310-18.